

High Temperature Cyclic Oxidation of Ti-Al Based Intermetallic in Static Laboratory Air

Astuty Amrin*, Esah Hamzah, Nurfashahidayu Mohd Badri and Hafida Hamzah

Department of Materials Engineering, Faculty of Mechanical Engineering,

81310 UTM, Johor, Malaysia

Email <astuty@fkm.utm.my>

Abstract— The objective of this study is to investigate the oxidation behavior of binary γ -TiAl based intermetallic; with composition (at%) of 45Al, 48Al and 50Al, and ternary alloys of Ti-48Al containing 2Cr and 4Cr. Thermal cyclic oxidation was conducted discontinuously at temperatures of 700°C and 900°C in static laboratory air. Optical microscopy, Scanning Electron Microscopy (FESEM), Energy Dispersive X-ray Analysis (EDX) and X-ray diffraction (XRD) techniques were employed for the analysis. SEM examination of cross-sectional samples using secondary electron and line-scan analysis after exposure at 700°C showed that non-adherent oxides scales formed due to the spallation caused by cyclic condition. While, exposure at 900°C, only binary alloys exhibited breakaway oxidation while the oxides scale formed on the ternary alloys were well-adhered on the substrate alloy. Overall, exposure at 900°C resulted in thicker and harder oxide scales and addition of Cr believed to improve oxidation resistance of Ti-Al based intermetallics at higher temperature.

1. Introduction

Ti-Al based intermetallic compounds based on are very light (low density), relatively stiff (high modulus), high resistance to hydrogen absorption, better mechanical behaviors with temperature and higher oxidation resistance. Thus, this materials is viable to replace some of the nickel-based alloys for applications at temperature up to 900°C. This intermetallics also has a high potential in advanced structural applications; such as aircraft system, high temperature moving parts and advanced transport systems such including planes and next generation engines.

Previous studies have showed that different composition of aluminum and the addition of other materials namely Cr, Nb, Sb, Ag, Si and halogens such as Cl and F resulted in different oxide scales formation. The scales may contain typical TiO₂ layer, mixed TiO₂ and Al₂O₃ layer and protective alumina scales with different length. Also the surface morphology was different for each various addition and composition of the materials at certain temperature and environment.

In this study, the oxidation behavior of binary and Cr containing TiAl-based alloy were investigated in thermal cyclic condition at 700°C and 900°C.

2. Experimental Procedures

Specimens were cut into dimensions of approximately 10mm x 10mm x 1mm using wirecut CNC machine and ground to 600 grit surface finish. The specimens were then cyclic oxidised in the high temperature oxidation tube furnace (Euroterm 2416CG) for 50 cycles. Each cycle consisted of heating to 700°C for about 152 minutes, holding at this temperature for 1 hour and cooling to room temperature for another 142 minutes. After the oxidation test, surface morphology test was evaluated by using FESEM and EDX (SUPRA 35VP). The composition of the oxide scales formed were analyzed by XRD (Siemens-D5000). Shidmazu HMV-2 Micro Hardness Tester was employed to determine the microhardness test across the cross-section of the specimens. Composition and the microhardness of the as-received samples are tabulated in **Table 1**.

Table 1. Compositions and microhardness of the as-received sample.

Sample	Ti	Al	Cr	Microhardness (Hv)
Ti-45Al	55.71	44.29	-	378
Ti-48Al	51.21	48.79	-	346
Ti-50Al	47.21	52.79	-	208
Ti-48Al-2Cr	49.38	48.65	1.98	260
Ti-48Al-4Cr	47.86	48.02	4.12	283

3. Results and Discussion

3.1. Oxidation Kinetics

The oxidation curves of weight gain per unit area under defined cyclic oxidation after exposure at 700°C in static laboratory air are illustrated in **Figure 1**. Curves for specimens Ti-50Al and Ti-48Al-2Cr exhibit a fluctuating trend indicating loss of weight change due to spallation rate and oxide scale re-growth rate. After 10 cycles the first spallation occurred to Ti-48Al-4Cr. The oxidation rate increased linearly after 10 cycles before decreasing between 10 to 40 cycles. The oxidation of Ti-48Al-2Cr was lower than Ti-48Al-4Cr after 20 cycles. The higher Al content and addition of Cr appeared to slow down the spallation in the case of cyclic oxidation at 700°C. The lowest weight change was recorded by sample Ti-48Al-4Cr with 0.028mg/cm² and Ti-48Al obtained the highest weight change loss with 0.06mg/cm² after 50 cycles of exposure. At this temperature, there is not much variation in the oxidation response of all the alloys. All

the binary and ternary alloys exhibit nearly the same parabolic behavior when oxidized in air at this temperature.

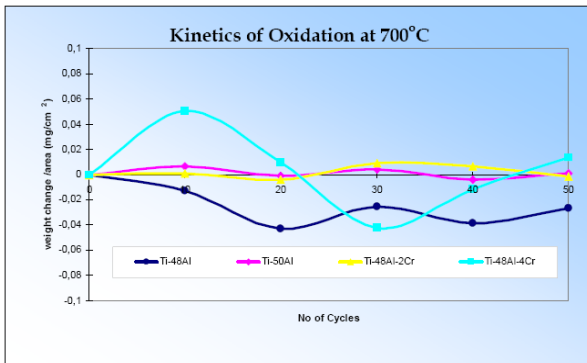


Figure 1. Weight change/area (mg/c m²) at 700°C

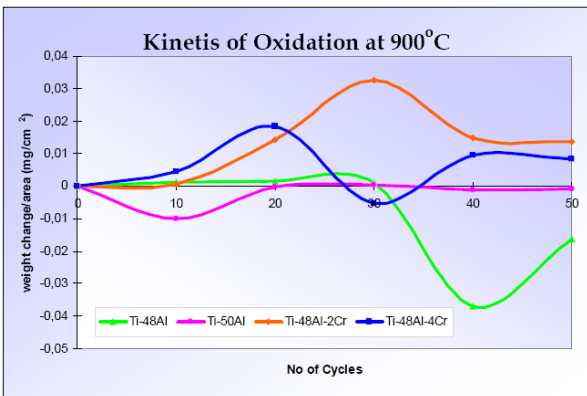


Figure 2. Weight change/area (mg/c m²) at 900°C

Figure 2 shows the oxidation kinetic after 50 cycles thermal cyclic exposure at 900°C in laboratory. The binary alloy of Ti-48Al and Ti-50Al showed the highest weight losses of -0.0037mg/cm² and 0.00023mg/cm² respectively. The plotted curves of Ti-50Al decrease after 30 cycles and continue increase with parabolic behavior curves after 20 cycles until end of cycles. During the first 10 cycles, the oxidation rate for Ti-48Al-2Cr going up rapidly but suddenly decreasing after 30 cycles. Ti-48Al-4Cr show similar behavior and at the same time loss weight of 0.0054mg/cm² because of spallation and re-growth. The oxide scale formed could not well-adhered on the surface in thermal cyclic condition de to cracking and spallation.

3.2. Surface morphology at 700°C

After 50 cycles exposure time at 700°C the slow oxidation rate due to incomplete diffusion process and lack of energy to transform metals ion from interface to the surface layer lead to formation of very tiny thin scale. From the EDX spectrum, Ti-48Al was rich with Al and believed to be alumina. In Ti-50Al and ternary alloys, the crystals were relatively finer and longer which looked like well-distributed ‘whiskers’ (Figure

3). The ‘whiskers structure is detected as TiO₂ in form of fine oxide were formed and distributed uniformly. Thicker oxides are form on alloy containing 4% Cr compared to other alloy. The crystal structures for ternary alloys were rather dense and larger in size.

In binary alloys, ‘cluster’ block crystal and long ‘whiskers’ type of oxide can be seen. From EDX analysis the ‘whiskers’ crystal were essential rutile-TiO₂ and the ‘cluster’ were mixture of Al₂O₃ and TiO₂ oxides. Both ternary alloys were dominated by ‘whiskers’ crystal or the rutile-TiO₂. The presence of Cr results in improvement of the TiO₂ oxidation rate and the scale grow rapidly on mixed Al₂O₃ and TiO₂ layer. From XRD analysis peaks of γ-TiAl and α₂-Ti₃Al was detected on both binary and ternary. Compound of Fe also have been detected on the surfaces.

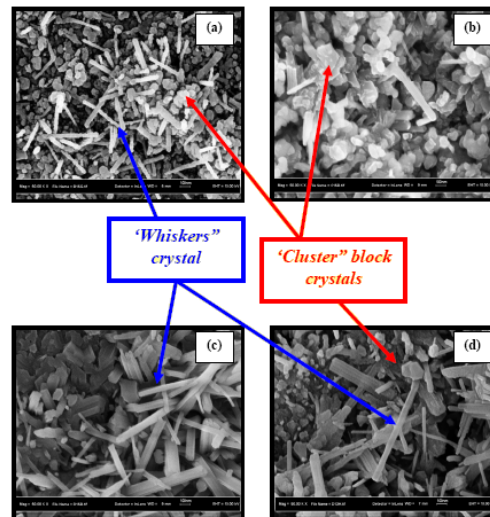


Figure 3. Surface morphology by FESEM after oxidation at 700°C and 50 cycles. (a) Ti-45Al, (b) Ti-48Al, (c) Ti-50Al, (d) Ti-48Al-2Cr, (d) Ti-48Al-4Cr

Cross-sectional analysis by FESEM shows a significant formation of oxide scale formed clearly. Due to spallation, the formation scale on Ti-50Al and Ti-48Al-4Cr are non-adherent. Generally, formations of oxide were thin at 700°C oxidation compared to 900°C. The compositions and structures of the scales were the same for all alloys. The EDX line-scan spectrum show that the outer part of the oxide scales contains mainly TiO₂ and the fraction of the outermost scale were detached. Figure 4 shows the cross-sectional micrograph of Ti-48Al with corresponding of EDX line-scan analysis after oxidation at 700°C for 50 cycles. Development of oxide scale depends on parameter of temperature and cyclic loading. The thickness of oxide scale is 625.2nm up to 982.5nm before the spallation occurred.

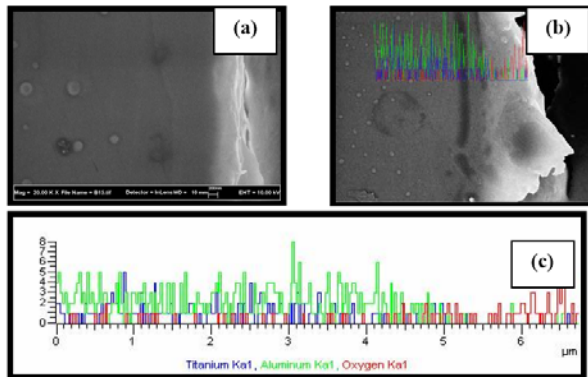


Figure 4. (a) Cross-sectional of Ti-48Al, (b) The cross-sectional with corresponding of EDX line scan analysis after cyclic oxidation at 700°C for 50 cycles, (c) EDX line-scan analysis of Ti-48Al.

3.3. Surface morphology at 900°C

The surface morphology of Ti-48Al after 50 cycles showed (Figure 5) the surface was completely covered by homogenous and a dense pillar-like rutile-TiO₂. The oxide scale of Ti-50Al formed under similar condition did not show any different from Ti-48Al. In both cases the surfaces were totally covered with pillar-like titania crystal without any indication of severe spallation of the oxide scales. While for Ti-48Al-2Cr and Ti-48Al-4Cr the surface morphology indicated severe spallation (Figure 6 and Figure 7). From the EDX analysis, the white particles found on the surface were rich in aluminum and oxygen as shown in Figure 6 (c) and (e). This phenomenon was the same in the case of Ti-48Al-4Cr whereby the EDX result (Figure 7 (e) and (f)) exhibit high intensity of TiO₂ in both examination. Cr containing alloys showed fast growing rutile covering the surface and occurrence of spallation while in binary alloy, the surface only covered by homogenous and dense scale of TiO₂.

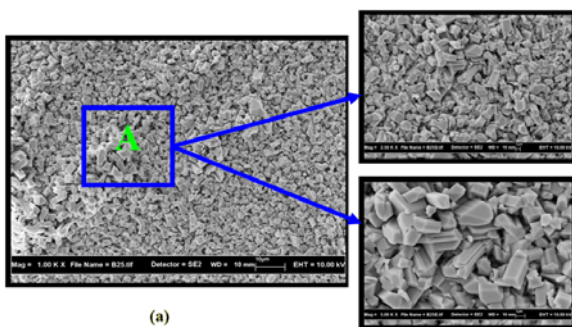


Figure 5. FESEM micrograph of Ti-48Al. (a) At 1000x, (b) 2500x, (c) 5000x

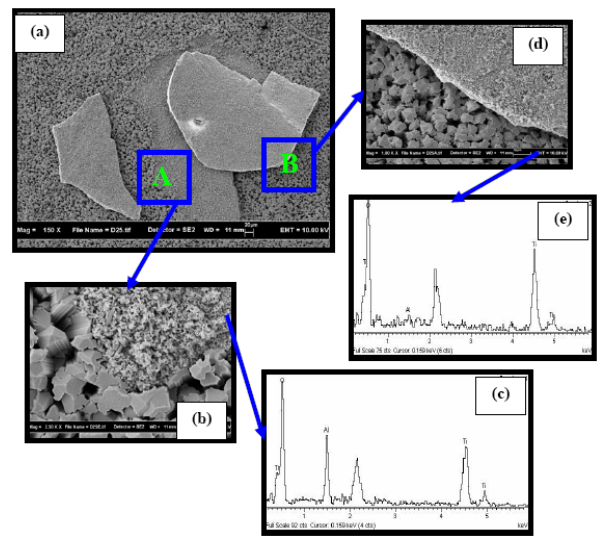


Figure 6. Surface morphology of Ti-48Al-2Cr, (a) At 150x, (b) Area A at 1000x, (c) Area B at 2500x, (d) EDX spectrum of spot A, (e) EDX spectrum of spot B.

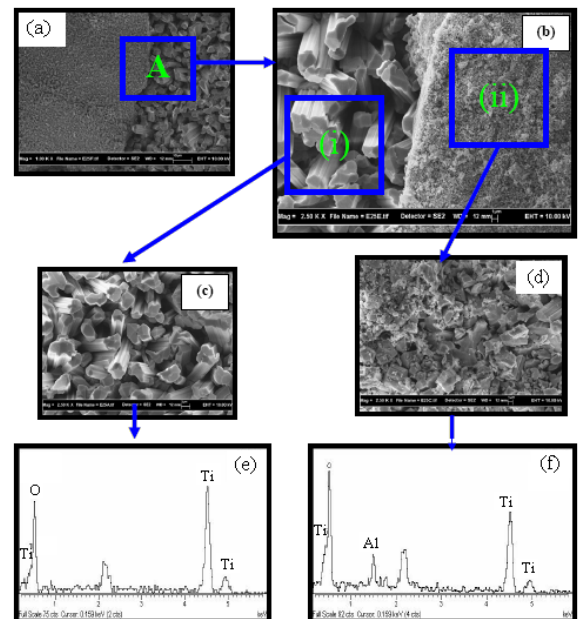


Figure 7. Surface morphology of Ti-48Al-4Cr, (a) At 1000x, (b) Area A at 2500x, (c) Area (i) at 2500x, (d) Area (ii) at 2500x, (e) EDX spectrum of spot (i), (f) EDX spectrum of spot (ii)

Apparently, cross-sectional analysis of oxidised specimens exposed at 900°C differ from 700°C for the same 50 cycles. Significant well adherent without any detachment of large oxide scale was clearly observed especially on the image of Ti-48Al-2Cr. The oxide scale was un-well adherent due to breakaway stage or because of the spallation. FESEM investigation did not show much different in Ti-48Al-2Cr and Ti-48Al-4Cr. The thickness for Ti-48Al-2Cr was 99µm and 112µm for Ti-48Al-4Cr. In case of ternary alloys, from the FESEM analysis the oxide scale is considerable as well-adherent to the alloy substrate compared to binary alloys. Detail investigation for

binary alloy Ti-50Al was showed after 50 cycles at 900°C (Figure 8).

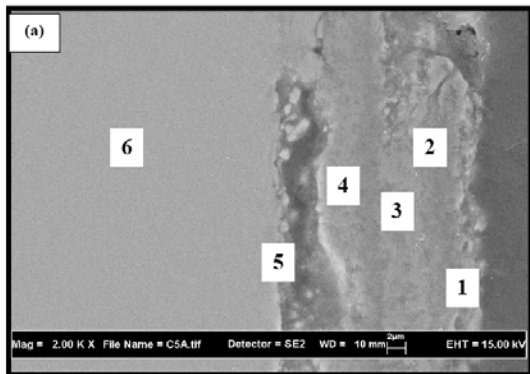


Figure 8. Cross-sectional of Ti-50Al after cyclic oxidation at 900°C for 50 cycles.

From EDX analysis it was found that the outer surface of region 1 contained mainly Ti and O (thickness: ~1µm). On the outer side of the oxide scale, a rutile-rich layer was found. The oxide formed showed an adherent layer without any detachment of large oxide particles. The inner part of this layer also Al-rich oxide particles were identified (dark particles) (thickness: ~0.8µm). Below this layer a semi-continuous aluminum-rich layer was detected (region 2) with a rather porous structure on the outer side. In this phase an oxide layer rich in aluminum had formed. Region 3 (thickness: ~1.6µm) consisted of banded regions with the bright ones rich in titanium and the darker rich in aluminum. Furthermore, it was found that the concentration of chromium was relatively high in the darker bands. At the inner side of this layer a porous structure was found (thickness: ~2.4µm). From this observation, it shows that the Ti-50Al oxide scale was non-adherent. Large areas on the surface showed significant spallation on region 4 (thickness: ~2.4µm). Region 5 (thickness: ~5µm) shows a remarkable low aluminum concentration (aluminum-depleted zone) and also close to the bulk value. A sharp interface could be detected between the bulk material and the formed corrosion scale. Region 6 corresponds to the bulk material. The total scale development scale was about 10.8µm. Composition on each region was shown in Table 2.

Table 2 Composition in Ti-50Al layer correspond to Figure 8.

Region	Ti(at.%)	Al(at.%)	O(at.%)	Remarks
1	68.07	10.48	21.45	Essential TiO ₂
2	70.82	5.66	23.51	Al ₂ O ₃ -rich layer
3	63.86	27.96	8.35	TiO ₂ -rich layer
4	68.56	7.06	24.38	Al ₂ O ₃ & TiO ₂ mixed layer
5	46.52	53.48	-	Al-depleted zone
6	46.36	53.64	-	Based-alloy

3.4. Mechanical Behavior

From the microhardness test, the ternary alloy showed higher value than binary alloys with Ti-48Al-4Cr show the highest value. The Cr content promoted the TiO₂ formation which was harder layer compared to others. The value of microhardness of the interface near to oxide scale relatively high for all 4 alloys. The values of microhardness begin to decrease rapidly at the substrate within interface and the base metal. This phenomenon distinguish that outward diffusion of Al occur at the substrate to react with oxygen and lead to formation soft layer of Al₂O₃. At the base alloy-oxide interface diffusion of Al or Al-depleted region tends to reduces hardness and sufficient to cause significant loss of ductility.

4. Conclusions

1. All binary and ternary alloys exhibit fluctuations curves after cyclic oxidation at temperature of 700°C and 900°C up to 50 cycles indicating non-protective behavior. The presence of Cr in ternary alloys demonstrates fastest oxidation rates with parabolic behavior at 900°C. After 20 or 30 cycles, weight change decreased dramatically and the phenomenon believed to due to spallation at both temperatures.
2. Surface morphology examination using FESEM revealed that mixed oxides formed with ‘whiskers’ crystal of TiO₂ and ‘cluster’ block of Al₂O₃ crystal exposed at temperature of 700°C. While at 900°C pillar-like TiO₂ crystal structure indicating that at high temperature, outward diffusion of Ti is faster leading to formation of TiO₂ covering the entire surfaces especially in binary alloys.
3. At both temperature, after 50 cycles, all the alloys formed non-adherent scale especially for ternary alloys at 900°C exposure. Thus, addition of Cr improves oxidation resistance at higher temperature.
4. XRD spectra show that the oxide scales consisting TiO₂, rutile-TiO₂ and nitride compound of Ti(NO₃)₄, after 900°C exposure. While at 700°C, the peak detected underlying intermetallic matrix of γ-TiAl, Ti₃Al and traces of Fe.

Acknowledgments

The authors are grateful to the Ministry of Higher Learning for the FRGS grant to support this research, and to IRC, University of Birmingham for preparing the titanium aluminides.

References

- [1] Astuty Amrin (2005). High Temperature Oxidation of Titanium Alumindes.
- [2] A. Amrin, E. Hamzah, F.H. Stott and G.C. Wood (2004). Oxidation behavior of Ti- Al at 900°C: Isothermal and Cyclic condition, Regional Conference and Workshop on Solid State Science and Technology, RCWSST, Kota Kinabalu, Sabah.
- [3] A. Amrin, E. Hamzah, F.H. Stott and G.C. Wood (2004). Oxidation behavior of Ti-Al based Intermetallic at 700°C and 900°C in flowing dry air, National Conference on Science and Technology, NACET, KL.
- [4] S. Thirumaran (2006). A Study of Scale Development On High Temperature Isothermal Oxidation of Titanium Aluminide In Flowing Dry Air
- [5] Djanarthany et. al. (2001). An overview of monolithic titaniumaluminides based on Ti₃Al and TiAl. *Materials Chemistry and Physics*, Vol:72, pp: 301-319.
- [6] J. D. Sunderkötter, H. J. Schmutzler, V. A. C. Haanapel, R. Hofman, W. Glatz, H. Clemens and M. F. Stroosnijder (1997). The High Temperature Oxidation Behavior of Ti-47Al-2Cr-0.2Si and Ti-48Al-2Cr-2Nb Compared with Ti-48Al-2Cr. *Intermetallics*, Vol. 5, pp: 525-534.
- [7] S. A. Kakare, P. B. Aswath (1997). Oxidation of TiAl Based Intermetallics. Materials Science and Engineering Program and Mechanical Aerospace Engineering, Department, University of Texas at Arlington, Arlington USA. *Journal of Material Science* 32, pp: 2485-2499.
- [8] S. C. Huang and J. C. Chestnutt (1995). Gamma TiAl and It's Alloys. *Intermetallic Compound*, Vol. II, ds: J. H. Westbrook and R. L. Fleicher. New York: John Wiley and Sons, pp: 73-90.
- [9] V. A. C. Haanapel, J. D. Sunderkötter, M. F. Stroosnijder (1999). The Isothermal and Cyclic High Temperature Oxidation Behavior of Ti-48Al-2Mn-2Nb compared with Ti-48Al-2Cr-2Nb and Ti-48Al-2Cr. Institute for Advanced Materials Ispra Site, Joint Research Centre of The European Commission. I-21020 Ispra (Va), Italy.
- [10] Mu Rong Ynag and Shyi-Kaan Wu (2003). Oxidation Resistance Improvement of TiAl Intermetallics Using Surface Modification. Taiwan.
- [11] J. R. Nicholls and M. J. Bennet (1995). Cyclic Oxidation-guidelines For Test Standardization, Aimed At The Assessment of Service Behavior. United Kingdom. 56-21
- [12] J. L. Murray (1987). *Phase Diagrams of Binary Titanium Alloys*. ASM International Metals Park, OH.
- [13] Mars G. Fontana, Norbert D. Greene (1998). *Corrosion Engineering*. Mc Graw-Hill International.
- [14] Per Kofstad (1998). *High Temperature Corrosion*. Elsevier Applied Science.
- [15] G. Lutjering, James C. Williams, Gerd Ltjering (2003). *Titanium*. Springer-Verlag Berlin Heidelbergh, New York.
- [16] G. Kubaschewski and Dr. Phil Habil (1993). *Oxidation of Metal and Alloy*. Principal Phisycal Laboratory, Butterworths Scientific Publication.
- [17] Gerhard Saufthuff (1995). *Intermetallic*. Weiheim, New York.
- [18] J. M. West (1986). *Basic Corrosion and Oxidation* 2nd Edition. Ellis Horwood Limited.